Springer

KSME

Journal of Mechanical Science and Technology 29 (7) (2015) 2803~2815
www.springerlink.com/content/1738-494x(Print)/1976-3824(Online)
DOI 10.1007/s12206-015-0609-9

Statistical calibration of a finite element model for human middle ear †

Dooho Lee[1,*] and Tae-Soo Ahn[2]

[1]*Department of Mechanical Engineering, Dongeui University, 995 Eomgwangno, Busanjin-gu, Busan, 614-714, Korea*
[2]*SEGI Engineering Inc., Byeoksan Digital Valley 712, 303 Daedong-ro, Sasang-gu, Busan, Korea*

(Manuscript Received October 27, 2014; Revised February 24, 2015; Accepted March 24, 2015)

Abstract

A Finite element (FE) model of a human middle ear is developed, assessed, and updated using a statistical approach. The model consists of three ossicles (malleus, incus, and stapes), a tympanic membrane, tendons, and ligaments. The uncertainty of the model input parameters associated with the material properties and boundary conditions are considered in order to assess the validity of the model. The variation of the umbo displacement transfer function (UDTF) as a result of the uncertainty of the model input parameters is estimated and compared with those from experiments. Using the analysis of variance (ANOVA) with a three-level orthogonal array, the most important calibration parameters, which are composed of stiffness-related and density variables, are selected. Furthermore, a metric for statistical calibration is introduced. Through minimizing the calibration metric, the calibration parameters are updated in order to enhance the performance of the middle ear FE model. The proposed statistical calibration framework effectively improves the middle ear FE model performance.

Keywords: Sound transfer function; Middle ear; Statistical calibration approach; FE model validation

1. Introduction

A key function of the human middle ear is to transfer sound energy from the air into the cochlear fluid of the inner ear so that the hair cells in the inner ear can generate the neuronal signals. Identifying the dynamic characteristics of the middle ear is very important in many areas including hearing aids, hearing loss evaluation, and design of middle ear prostheses. Many experimental measurements have been conducted in order to understand the dynamics of the middle ear [1, 2]. The dynamic characteristics of the middle ear exhibit a very complex behavior as well as individual variations. Experiments on live humans and cadavers are very limited, which indicates a need for a valid numerical model of the middle ear in order to simulate the changes of transfer functions according to, for example, the designs of middle ear prostheses. However, the numerical models in a computer have numerous uncertainties, which lead to large uncertainties in the simulated middle ear dynamic characteristics. Therefore, an effective methodology is required in order to quantify these uncertainties and to estimate the validity of the numerical models.

For the numerical analysis of the middle ear dynamic characteristics, there are two types of model: network models and geometry-based models. Network models use an analogy between the vibro-acoustic components in the middle ear and electric components such as inductors, resistors, and capacitors [3]. Network models predict the sound transfer function using only a few parameters; however, network models have limitations because the lumped parameter model cannot avoid intrinsic difficulty in determining the model parameters equivalent to the complex geometry in the middle ear. Geometry-based models are constructed from a discretization of geometry of the middle ear. Among the geometry-based models, the finite element (FE) method has been used to calculate the dynamic characteristics of the middle ear as a result of the rapid advances in computation power and geometric modeling technologies [4-7]. Recently, geometric modeling techniques have enabled accurate modeling of the middle ear sufficient for high frequencies using high resolution computed tomography (CT) or magnetic resonance imaging (MRI) scanning of the middle ear [8]. However, there are only a few specimens available for the material properties of the middle ear including the ossicles, ligaments, tendons, and muscles, and these have large variations and uncertainties. The uncertainties cause finite element models of the middle ear to encounter difficulties in accurately predicting the sound transfer characteristics. In different FE models of the human middle ear, the material properties of the FE models exhibit large differences in magnitude as noticed in Ref. [9]. The authors [9, 10] developed a finite element model for a middle ear that was based on the high-precision geometry data and material properties from

*Corresponding author. Tel.: +82 51 890 1658, Fax.: +82 51 890 2232
E-mail address: dooho@deu.ac.kr
† Recommended by Associate Editor Moon Ki Kim

published articles. The performance of the developed FE model exhibited good agreement in the low frequency bands, but it deviated from the measurement data in the high frequency bands. Thus, it is necessary to quantitatively estimate the validity of the developed FE model and to update the FE model for better performance in the high frequency bands.

The validation can be defined as the process of determining the degree to which a numerical model is an accurate representation of the real world from the perspective of the intended uses of the model [11]. To appropriately assess the performance of the numerical model, the uncertainties and errors should be statistically quantified and a proper metric that represents the agreement between the numerical model and experimental data should be introduced. The statistical calibration or updating of the numerical model can also be defined as the refining the prior distributions of a set of input parameters for the numerical model in order to maximize the agreement between the results of the numerical model and a chosen set of experimental data [12, 13]. The validation and calibration of a numerical model under data and model uncertainties are ongoing issues in many areas [14, 15]. The validation scheme can be adaptively changed according to the situation, e.g. the problem principles and available data. The verification and validation of numerical models in biomechanics have been reviewed in Refs. [16] and [17]. Recently, the authors [18] explored the validation and updating for an acoustic boundary element model of a human outer ear using a statistical approach and response surface method; this research is now being extended to the developed FE model of the middle ear.

In this study, the validity of the FE model for a middle ear is quantitatively estimated using statistical percentiles estimation and a novel validation metric. The input parameters of the FE model that have a significant influence on the tympanic membrane responses are also updated using an optimization technique with two different model error formulations. In Sec. 2, the FE model of the middle ear is explained. Sec. 3 presents a statistical validation approach for the FE model of a middle ear using a validation metric. In Sec. 4, the model updating scheme is explained. Furthermore, the most appropriate values of the calibration parameters are identified using an optimization formulation after selecting the calibration parameters from the input parameters. In Sec. 5, the proposed approach is summarized.

2. FE model of the middle ear

The authors developed an FE model for the middle ear of a Korean subject [9, 10]. The FE model can predict the vibro-acoustic transfer function of the middle ear from the tympanic membrane to the entrance of the cochlear fluid. As state in Introduction section, the performance of the FE model shows good agreement in the low frequency bands, but low agreement in the high frequency bands. This study aims to develop a procedure of statistical model calibration based on the existing FE model for human middle ear and experimental data.

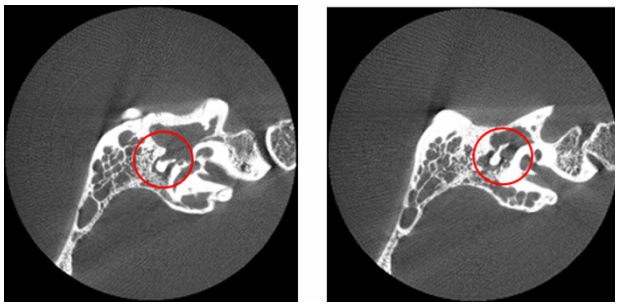

(a) Slice images of the temporal bone

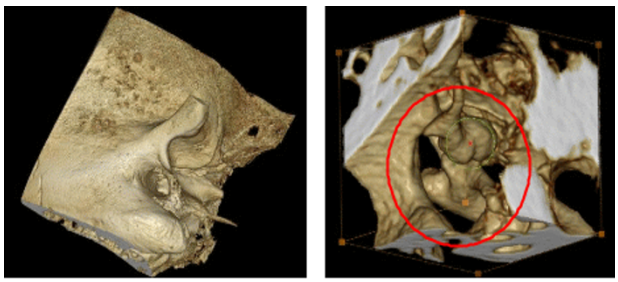

(b) Reconstructed 3D temporal bone

Fig. 1. Slice images from the micro-CT scanning and reconstructed geometry for the temporal bone.

Thus, the FE model is briefly explained in this section. For more details on the FE model, refer to Refs. [9] and [10].

2.1 Geometric modeling of ossicles

The precise geometry of ossicles was obtained through micro-CT scanning of the temporal bone of a Korean cadaver. The micro-CT scanning resolution was 0.12 mm with 5123 voxels. The two-dimensional slice images were transformed into three-dimensional solid geometries of the three ossicles using post-processing software (3D-DOCTOR, Version 3.5; Able Software Corp., USA). Fig. 1(a) presents representative slice images from the micro-CT scanning of the temporal bone. The slice images were stacked in order to reconstruct the three-dimensional geometry of the ossicles as shown in Fig. 1(b). The ossicles were restrained by the tympanic membrane, ligaments, tendons, and muscles on temporal bone.

These restraints, which critically affect the mechanical motion of the middle ear, were considered in the FE modeling of the middle ear. For the modeling, the tympanic membrane geometry was generated as a surface from the published data, of which thickness was taken from Ref. [5]. The other elements including the ligaments, tendons, and muscles were attached to the ossicles and tympanic membrane according to the anatomical structure of the middle ear.

2.2 Finite element (FE) modeling

The geometry generated for the middle ear was discretized into finite elements. The FE model consisted of 4949 nodes

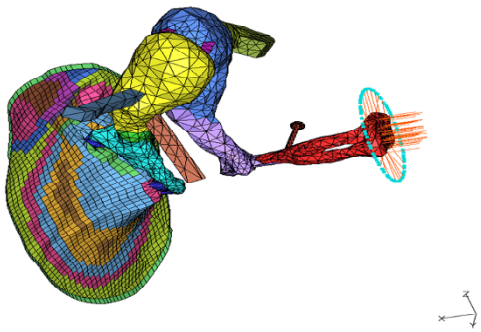

Fig. 2. FE model of the middle ear.

and 13926 elements. Fig. 2 presents the FE model of the middle ear and its boundary conditions. As shown in Fig. 2, the ossicles were modeled using solid elements and the tympanic membrane was modeled as shell elements. The other elements such as ligaments, tendons, and muscles were represented as solid elements. Two joints in the ossicles (i.e. incudomalleolar (IM) joint and incudostapedial (IS) joint) heavily influence the dynamic behavior of the middle ear; these joints were modeled using solid elements. The shapes of the joints, ligaments, tendons, and muscles were determined based on the micro-CT data and the anatomical auditory structure. The effects of the cochlea were considered as the boundary condition of the stapes footplate: the cochlear fluid was modeled using linear springs and viscous dashpots.

The material properties used in the FE model are taken for Ref. [9] and summarized in Table 1. Using the FE model, the frequency response functions of the middle ear were calculated. The umbo displacement transfer function (UDTF) was defined as a frequency response function of the umbo displacement due to the unit sound pressure on the tympanic membrane. In order to calculate the UDTF using the FE model, the nodal displacements of the nodes in the umbo region of the tympanic membrane were averaged when a unit sound pressure was applied on the tympanic membrane in the frequency domain. Thus, the UDTF is defined as follows:

$$G = 20\log_{10}\left(\frac{y_u}{1.0\times10^{-6}\ m/Pa}\right) \quad (1)$$

where y_u is the averaged displacement transfer function of the umbo region. The displacement transfer functions in this study were calculated using commercial software, MSC/NASTRAN with the direct frequency response solution method.

The UDTF was calculated using the FE model with the material properties described in Table 1. Fig. 3 presents the UDTFs calculated using the FE model from 100 Hz to 10 kHz. The calculated UDTFs were compared with those of the measurements in Ref. [19]. The experimental results that were measured from 99 human ears were expressed as the mean, 10 percentile, and 90 percentile values for each frequency. In Fig. 3, it can be seen that the FE model represents the dynamic

Table 1. Material properties of the middle ear FE model [9].

Composition		Young's modulus (N/m^2)	Density (kg/m^3)	Mass (mg)	Remarks
Tympanic membrane(TM)	(Tensa)	3.34×10^7	1.2×10^3	6.52	
	(Flaccida)	1.11×10^7	1.2×10^3	0.89	
Malleus	(Head)	1.2×10^{10}	2.55×10^3	19.36	
	(Neck)		4.53×10^3	2.43	
	(Handle)		3.70×10^3	4.28	
Incus	(Body)	1.2×10^{10}	2.36×10^3	21.6	
	(Short process)		2.26×10^3	3.66	
	(Long process)		5.08×10^3	5.49	
Stapes		1.2×10^{10}	2.2×10^3	3.056	
Incudomalleolar(IM) joint		1.2×10^{10}	3.2×10^3	1.97	
Incudostapedial(IS) joint		4.3×10^5	1.2×10^3	0.056	
Anterior mallear ligament		4.6×10^6	2.5×10^3	0.86	
Posterior incudal ligament		6.5×10^5	2.5×10^3	2.96	
Tensor tympani muscle		2.6×10^5	2.5×10^3	0.49	
Manubrium		4.7×10^9	1.0×10^3	0.18	
Stapedius muscle		5.2×10^5	2.5×10^3	0.07	
Tympanic annular ligament		6.0×10^5	2.5×10^3	2.5	
Total			-	76.33	
Stapedius annular ligament		9 N/m			
Cochlear fluid		k = 70 N/m, C = 0.054 Ns/m			42 springs
Loss factor		0.5			Overall damping for all structural elements
Poisson's ratio		0.3			For all structural elements

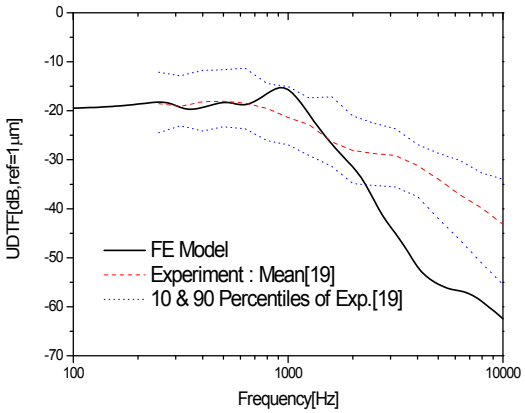

Fig. 3. Umbo displacement transfer function compared with those in the experiments.

behavior of the UDTF of the human ear well below 2 kHz. However, the UDTF of the FE model gradually deviates from the experimental results in the higher frequency regions above 2 kHz. The reasons for this disagreement in the UDTF in high frequency regions are uncertain: they could originate from FE model errors, uncertainties of the material properties, and/or experimental errors as discussed in Ref. [18]. In order to assess the FE model appropriately, these errors and the variability of the UDTF due to the input uncertainties of the numerical model must be quantified. Thus, the validation of the FE model is necessary and is conducted in Sec. 3.

3. Statistical validation of the FE model

Validation is defined as the process of determining the degree to which a numerical model is an accurate representation of the real world from the viewpoint of the intended uses of the model [11]. In some situations, the validation includes calibration or model updating, which typically involves adjusting the selected model parameters in order to maximize the agreement of the numerical model output with the empirical observations [15]. However, in this paper, the terminology is confined to the process of assessing the numerical model accuracy through comparisons of the predictions against the experimental data.

The numerical model has uncertainties in the model input parameters, and these parameter uncertainties propagate into the predictions through the numerical model. Thus, the input parameter uncertainties and propagated uncertainties in the system responses of interest should be quantified. Then, the model accuracy can be assessed quantitatively with the introduction of an appropriate validation metric.

3.1 Uncertainty sources of the FE model

A numerical model has various uncertainty sources such as model form, input parameters and numerical approximations [20]. The model inputs for a numerical model are categorized into two types: controllable parameter ($\mathbf{x}$) and uncontrollable parameter ($\boldsymbol{\theta}$). In the numerical model, the controllable parameter has no uncertainty and, thus, can be treated as a deterministic value. The uncontrollable parameter has uncertainty of which reason is due to inherent nature in a quantity or lack of knowledge. A probabilistic distribution, regardless of which represents frequency of occurrence or degree of belief, can describe the uncertainty of the uncontrollable parameters. The classification of input parameters depends on the problems being treated. When an input parameter is precisely known or variability is negligible, the parameter can be categorized into the controllable parameter. In this study, it is assumed that the controllable input parameter is always deterministic. The uncontrollable input parameters are assumed to have uncertainties in their values.

In a non-deterministic approach, the relationship between the physical experiments and FE model outputs can be formulated as follows [14, 15]:

$$y^e(\mathbf{x}) = y^m(\mathbf{x}, \boldsymbol{\theta}) + \delta(\mathbf{x}) + \varepsilon \,, \tag{2}$$

where $\mathbf{x} = \{x_1, x_2, \ldots, x_n\}$ are the controllable input parameters, $\boldsymbol{\theta} = \{\theta_1, \theta_2, \ldots, \theta_q\}$ are the uncontrollable input parameters, $y^e(\mathbf{x})$ is the measurement data, $y^m(\mathbf{x}, \boldsymbol{\theta})$ is the FE model output, $\delta(\mathbf{x})$ is a bias FE model error, and ε is the measurement error. The bias FE model error, $\delta(\mathbf{x})$, represents errors due to mathematical formulation, assumptions and approximations that are used in the FE model: for example, errors due to nonlinearities of tympanic membrane material. It should be noted that the uncontrollable parameters are treated as random variables in calculating the FE model outputs in the uncertainty propagation analysis of the next subsection. Uncertainties in the uncontrollable input parameters propagate into the predictions through the FE model. Thus, the FE model outputs have distributions: i.e., not a deterministic value but determined by a probabilistic process. In the validation process, the model errors and input uncertainties should be identified and quantified for the numerical model.

Measuring the mechanical properties of organic materials is very difficult and sometimes impossible due to the limited number of samples, small size, short shelf life, and so on. Furthermore, the environmental conditions of experimental equipment (i.e. humidity and temperature) easily influence the mechanical properties of the organic materials. Particularly with the middle ear components, the experimental measurements of the mechanical properties are very limited due to the small size of the organ [21-26]. Thus, the available mechanical properties of the middle ear have a large uncertainty. For example, the experimental estimation results for the Young's modulus of the human pars tensa from several researchers varied from 0.4 MPa to 56.8 MPa [25]. Therefore, the mechanical properties of the FE model should be considered as random variables: i.e., the uncontrollable input parameters. The geometry variations in the middle ear that occur from subject to subject might also be large, but the geometry of the FE model is considered deterministic in this study. This is because the geometry of the middle ear was modeled with high precision and the geometry uncertainty for this non-parametric shape was too complex to be considered. Note that the effects of disregarding the geometry uncertainties in the middle ear FE model are included as discrepancies (Model form errors) in the FE model that should be quantified in the validation process.

The FE model for the middle ear is a linear model that calculates the dynamic response of the tympanic membrane. As shown in Table 1, the mechanical properties of the FE model can be categorized into three types: stiffness, mass, and damping properties. The stiffness and damping properties are frequency-dependent in the linear model, whereas the mass properties are usually constant along the frequency axis. In the FE model explained in the previous section, the material properties were selected from the typical values currently known,

Table 2. Stiffness-related random variables selected for the FE model validation.

No.	Random variable (Stiffness value)	Mean	Standard deviation	Distribution type
1	Malleus	$\log_{10}(1.2\times10^{10})$	10% COV	Lognormal
2	Incus	$\log_{10}(1.2\times10^{10})$	10% COV	Lognormal
3	Stapes	$\log_{10}(1.2\times10^{10})$	10% COV	Lognormal
4	Incudomalleolar joint	$\log_{10}(1.2\times10^{10})$	10% COV	Lognormal
5	Incudostapedial joint	$\log_{10}(4.3\times10^{5})$	10% COV	Lognormal
6	Tympanic annular ligament	$\log_{10}(6.0\times10^{5})$	10% COV	Lognormal
7	Cochlear fluid	$\log_{10}(7.0\times10^{1})$	20% COV	Lognormal
8	Tympanic membrane (Tensa)	$\log_{10}(3.34\times10^{7})$	10% COV	Lognormal
9	Tympanic membrane (Flaccida)	$\log_{10}(1.11\times10^{7})$	10% COV	Lognormal
10	Structural damping	$\log_{10}(0.5\times10^{0})$	20% COV	Lognormal

Table 3. Density random variables selected for the FE model validation.

No.	Random variable (Density value)	Mean	Standard deviation	Distribution type
1	Tympanic membrane (Tensa, flaccida)	$\log_{10}(1.2\times10^{3})$	5% COV	Lognormal
2	Malleus (Head)	$\log_{10}(2.55\times10^{3})$	5% COV	Lognormal
3	Malleus (Neck)	$\log_{10}(4.53\times10^{3})$	5% COV	Lognormal
4	Malleus (Handle)	$\log_{10}(3.70\times10^{3})$	5% COV	Lognormal
5	Incus (Body)	$\log_{10}(2.36\times10^{3})$	5% COV	Lognormal
6	Incus (Short process)	$\log_{10}(2.26\times10^{3})$	5% COV	Lognormal
7	Incus (Long process)	$\log_{10}(5.08\times10^{3})$	5% COV	Lognormal
8	Stapes	$\log_{10}(2.2\times10^{3})$	5% COV	Lognormal
9	Incudomalleolar joint	$\log_{10}(3.2\times10^{3})$	5% COV	Lognormal
10	Incudostapedial joint	$\log_{10}(1.2\times10^{3})$	5% COV	Lognormal
11	Manubrium	$\log_{10}(1.0\times10^{3})$	5% COV	Lognormal
12	Ligaments (Anterior mallear, posterior incudal)	$\log_{10}(2.5\times10^{3})$	5% COV	Lognormal
13	Muscle (Tensor tympani, stapedius)	$\log_{10}(2.5\times10^{3})$	5% COV	Lognormal

but have large uncertainties associated with the ligaments, tendons, and muscles, as well as those of the ossicles. In order to quantify the input parameter uncertainties of the FE model, the mechanical properties were divided into two groups as shown in Tables 2 and 3: a stiffness-related group and a density group. All variables were assumed to be lognormal distributions of which the means were set to the logarithmic values of the deterministic values in Table 1. The standard deviations of the stiffness and density were assumed to be 10% and 5% coefficient of variation (COV), respectively, based on those of typical engineering materials. Particularly for the structural damping and cochlear fluid stiffness, the standard deviations were enlarged to 20% due to their large uncertainties. Tables 2 and 3 summarize the input parameter uncertainties for the FE model.

3.2 Uncertainty propagation analysis in the FE model

Because the uncertainties of the input parameters propagate into the system output of interest through the FE model, the responses calculated using the FE model become a distribution which can be represented using a probability density function (PDF). Here, the system output of interest in the middle ear FE model is the UDTF. Note that the experimental data available from the one particular paper was the means and two percentile values (10^{th} and 90^{th}) of the measured UDTF along the frequency axis. In order to assess the FE model based on the experimental data, the PDF of the UDTF should be obtained using a probability analysis. The PDF of the UDTF can be calculated using probability analysis methods including the Monte Carlo simulation(MCS) method and eigenvector dimension reduction (EDR) method [27]. With sufficient number of random samples (typically one million samples), the MCS method gives accurate probability information. However, the MCS method cannot be used in calculating the PDFs of large numerical models because of expensive computational cost. Thus, many approximation methods such as the EDR method have been developed.

The EDR method is a statistical moment-based method that uses the principal directions of the covariance matrix in order to approximate the statistical moments (i.e. mean, standard deviation, skewness, and kurtosis) of a system response and the moving least square approximation method. From the estimated statistical moments, the EDR method extracts its

PDF using the stabilized Pearson system equation. For N random variables, the EDR method only demands 2N+1 or 4N+1 samples to obtain the PDF of a system response. It has been demonstrated that the EDR method is accurate in calculating the PDF and reliability in structural-acoustic systems [28]. For further details on the EDR method, refer to Ref. [27]. In this paper, the EDR method developed as an in-house code under MATLAB environment was used with a 2N+1 sampling scheme in order to obtain the PDF of the UDTF that results from the parameter uncertainties of FE model.

The PDFs of the UDTF in the middle ear FE model were estimated for two cases: Case I is where only the uncertainties of the stiffness-related input parameters (i.e. the variables in Table 2) were considered in the variability analysis and Case II is where all uncertainties in Tables 2 and 3 were considered. Fig. 4(a) presents the PDF analysis results. In Fig. 4(a), the mean values of the UDTF in the FE model are plotted together with the 10% and 90% cumulative distribution function (CDF) values. For the experimental data, the mean values and 10^{th} and 90^{th} percentiles are also displayed. Note that the distribution type and PDFs were not available for the experimental data. Comparing the CDF widths between the 10% and 90% values with those of the experiments, the PDF calculation results in Fig. 4(a) exhibited similar tendencies in both cases: i.e. good agreement below the 2 kHz frequency band and lower responses than the measurements in the higher frequency band. Investigating the similar widths of the UDTF variabilities for both cases in Fig. 4(a), the stiffness-related group variables may have a larger influence on the variability of the UDTFs than the density variables. However, these results must be carefully interpreted because the variability widths can change according to the assumed standard deviations of the random variables. It should be noted that the variabilities of the density variables were assumed to be smaller than those of the stiffness-related variables, and the uncertainties of the statistical information such as the mean and variance are not yet known accurately. The variability widths of the measured CDFs for higher frequency region are narrower than those of the calculated ones in Fig. 4(a). The origin of this discrepancy can come from two sources: inaccurate estimated variabilities of the input parameters for the FE model and unknown variability sources that are not treated in this study. For the former cases, the statistical calibration approach of Sec. 4 can adjust the discrepancy, while not for the latter cases. The quantification of input parameter uncertainties is very crucial step in the statistical approach. Unidentified sources of the variability result in errors of the statistical calibration results: this is a general limitation of the inverse approach.

3.3 Statistical assessment of the middle ear FE model

In order to quantitatively assess the middle ear FE model, an appropriate validation metric should be defined [20, 29]. In this paper, the experimental UDTFs were obtained from the

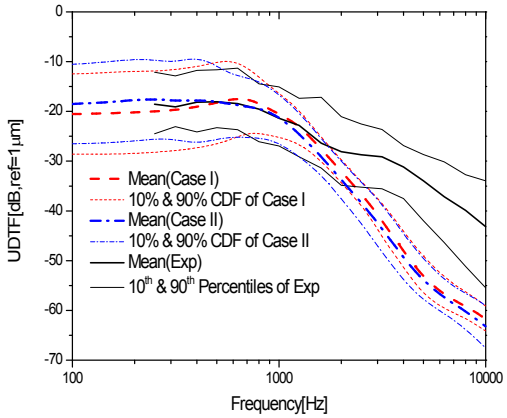

(a) Response variability

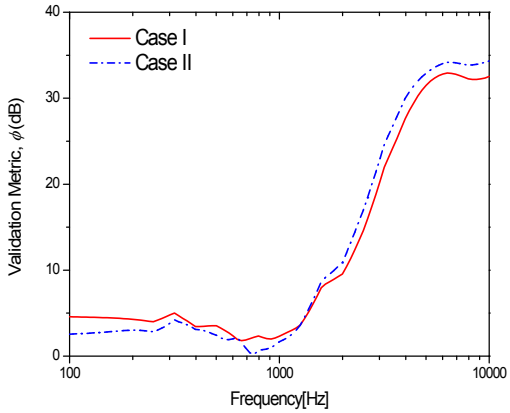

(b) Validation metric

Fig. 4. Variability analysis results for the FE model (Case I: stiffness-related variables only and case II: all variables).

published data in Ref. [19], which were obtained from 99 human subjects. Because only the mean values and 10^{th} and 90^{th} percentile values were presented in the reference, all PDFs of the UDTFs between the FE model and experiments could not be compared. Thus, a new validation metric was defined in order to compare the mean and two percentile values (10^{th} and 90^{th}) of the UDTF between the experiments and the calculated UDTFs, as follows:

$$\phi(f) = \left((G^m_{p_{10}} - G^e_{p_{10}})^2 + (G^m_{\mu} - G^e_{\mu})^2 + (G^m_{p_{90}} - G^e_{p_{90}})^2 \right)^{1/2}, \quad (3)$$

where f is the frequency, the superscripts m and e refer to the FE model and experiment, respectively, and the subscripts μ, p_{10}, and p_{90} are the mean, 10^{th} percentile (10% CDF), and 90^{th} percentile (90% CDF), respectively. The validation metric ϕ can be interpreted as the magnitude of a vector with three components that are the differences of the UDTFs between the FE model and experiments at a frequency.

Using the PDFs of the UDTFs that were obtained using the EDR method for the FE model in the previous subsection, the validation metrics were calculated and are plotted in Fig. 4(b)

for both cases. As shown in Fig. 4(b), the validation metric clearly illustrates that the middle ear FE model exhibits good agreement with the experimental data on the low frequency band, while on higher frequency region over 2 kHz, the UDTFs of the FE model have increasing errors (Discrepancies) with the experiments. Noting that in Fig. 4(a) the UDTF bounds from the 10% and 90% CDFs of the FE model and from the 10^{th} to 90^{th} percentiles of the experimental data do not have an intersection region if the frequency is larger than 2 kHz, it can be seen that the ϕ function is a good measure for representing the performance of the FE model.

The large values of the validation metric above the 2 kHz frequency band can be caused by the FE model errors and inaccurate estimations of the input parameters (i.e. mean and variance). In order to enhance the performance of the FE model, the distributions of the input parameters can be updated. The bias between the FE model and experiment should also be reduced. These activities require a calibration framework for the FE model, which is considered in the next section.

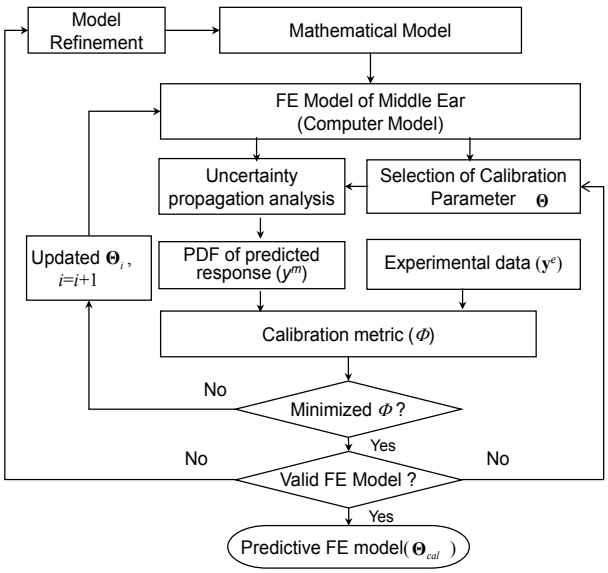

Fig. 5. Flowchart for the FE model calibration.

4. Statistical calibration of the FE model

The model calibration or updating process for a numerical model is a primary concern of numerous researchers regardless of whether the calibration is undertaken before the validation [15] or is included in the validation process [18]. The calibration process has been established overall, but for the detailed view there are numerous different strategies because there are numerous situations between a numerical model and the available experimental data in various areas. In this section, a calibration framework is introduced to enhance the performance of the FE model for the middle ear.

4.1 Calibration framework for the FE model

Calibration frameworks differ according to the problems and available reference data. In this study, the FE model outputs is updated (or calibrated) as follows:

$$y^{m'}(\mathbf{x},\Theta) = y^{m}(\mathbf{x},\boldsymbol{\theta}) + \delta(\mathbf{x}) + \varepsilon\,, \tag{4}$$

where $y^{m'}(\mathbf{x}, \boldsymbol{\Theta})$ is the updated FE model output, $\boldsymbol{\Theta}$ is the calibration parameter. The calibration parameter vector $\boldsymbol{\Theta}$ is composed of the distribution parameters of selected random variables ($\boldsymbol{\theta}_s$) among the uncontrollable input parameters $\boldsymbol{\theta}$, the regression coefficients of the FE model error, and the standard deviation of the measurement error. The measurement error (ε) was assumed to be a zero-mean Gaussian random variable. All uncontrollable input parameters in Sec. 3 were assumed to be lognormal distributions of which distribution parameters are mean and standard deviation. The FE model error $\delta(\mathbf{x})$ was assumed to be a deterministic function that can be regressed using a linear relationship with respect to the controllable input parameters $\mathbf{x}$, as follows:

$$\delta(\mathbf{x}) \cong \boldsymbol{\beta}_0 + \boldsymbol{\beta}_1^{T} \cdot \mathbf{x}\,, \tag{5}$$

where $\boldsymbol{\beta}_0 = \{\beta_{01}, \beta_{02}, \ldots, \beta_{0n}\}$ and $\boldsymbol{\beta}_1 = \{\beta_{11}, \beta_{12}, \ldots, \beta_{1n}\}$ are the linear regression coefficient vectors and n is the number of the controllable input parameters. Thus, the calibration parameter vector $\boldsymbol{\Theta}$ can be written as follows:

$$\boldsymbol{\Theta} = \left\{\mu_{\theta 1}, \sigma_{\theta 1}, \mu_{\theta 2}, \sigma_{\theta 2}, \cdots, \mu_{\theta r}, \sigma_{\theta r}, \beta_{01}, \beta_{11}, \cdots, \beta_{0n}, \beta_{1n}, \sigma_{\varepsilon}\right\} \tag{6}$$

where r is the number of the selected uncontrollable input parameters ($r \le q$), and μ and σ refer to the mean and standard deviation, respectively.

In order to enhance the performance of the FE model, the uncertainties of the selected uncontrollable input parameters should be updated and the FE model errors and measurement errors should be quantified. The calibration problems can be formulated as a minimization problem of a calibration metric (Φ), as follows:

$$\begin{aligned} &\textit{Find the calibration parameter } \boldsymbol{\Theta} \textit{ so as to that} \\ &\quad \textit{minimize } \Phi(\boldsymbol{\Theta} \mid \mathbf{x}) \\ &\quad \textit{subject to } \boldsymbol{\Theta}_L \le \boldsymbol{\Theta} \le \boldsymbol{\Theta}_U \end{aligned} \tag{7}$$

where $\boldsymbol{\Theta}_L$ and $\boldsymbol{\Theta}_U$ are the lower and upper bounds of the calibration parameters, respectively. Fig. 5 demonstrates the calibration framework used in this paper for the middle ear FE model. The calibration parameters were selected from the FE model input parameters. Then, they were updated so that the validation metric was minimized. The PDFs of the predicted response can be calculated using the EDR method in order to evaluate the validation metric. After minimizing the validation metric, the FE model was examined from the viewpoint of the validation metric, the quantified FE model error and measurement error. If the FE model is not satisfactory in its per-

formance, the calibration parameters can be reselected or the model can be refined, e.g. remeshing the FE model and/or redefining the mathematical model can be conducted as demonstrated in Ref. [12].

4.2 Selection of calibration parameters

The FE model of the middle ear has numerous uncertain input parameters. Generally, all uncertain input parameters cannot be used as calibration parameters due to the computational burden. The calibration parameters can be selected through estimating the influence of the input parameters on the system response. In order to estimate the influence of the input parameters, an analysis of variance (ANOVA) using an orthogonal array [30, 31] was conducted. In the ANOVA, the variance that resulted from each input could be calculated using the sum of squares and degrees of freedom. Then, the variance ratio of the i-th input (F_i) can be defined as follows:

$$F_i = \frac{V_i}{V_e}, \tag{8}$$

where V_i and V_e are the variances of the i-th input parameter and error, respectively.

Comparing the F values of the input parameters, the statistical significance of the input parameters can be evaluated [30].

F-tests were performed for the input parameters of the FE model. The first F-test was for the stiffness-related variables in Table 2. An L_{27} orthogonal array that can allocate 13 variables using three levels was introduced for the ANOVA. The input parameters were allocated in the orthogonal array. The three levels of each input parameter were set to μ–3σ, μ, and μ+3σ. Then, using a different set of the input parameters corresponding to each row of the orthogonal array, the UDTFs were calculated using the middle ear FE model. For the density input parameters in Table 3, the same procedure was repeated for the F-test. Fig. 6 presents the F-test results for the stiffness-related and density variables. The F-test value was normalized by the Euclidean norm of the all F-values on a frequency by frequency basis. Note that the magnitudes of the influence were frequency dependent.

For the stiffness-related variables, the stiffnesses of the tympanic membrane, annular ligament, malleus, and incus, and the structural damping were the most influential input parameters on the UDTF among all variables in Table 2. For the density variables, the densities of the tympanic membrane, malleus, and incus were the most dominant input parameters to the UDTF among all variables listed in Table 3. It should be noted that due to the location of the system response (i.e. at the umbo), compositions further from the response point generally could not have a significant influence, particularly in the high frequency range. The masses of the compositions in Table 1 were highly correlated to the degree of importance to the UDTF in almost all frequency ranges for the density variables. The density parameter of the joints exhibited a large influence

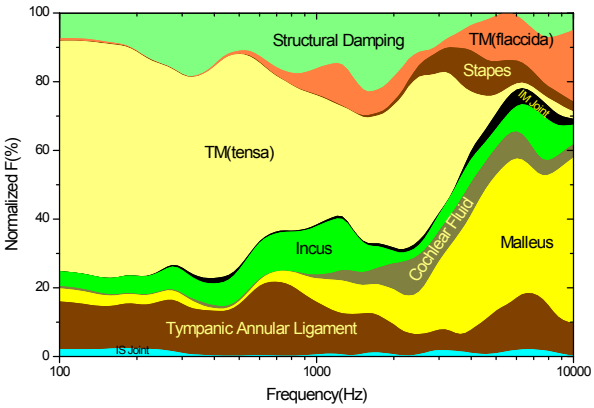

(a) Stiffness-related variables

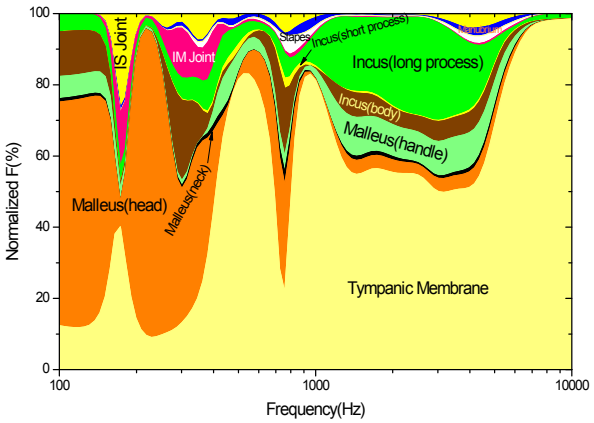

(b) Density variables

Fig. 6. ANOVA results for the FE model.

on the UDTF in narrow frequency ranges. However, for the joints, the updating of the stiffness rather than the density is more appropriate because the joint masses were very small, as shown in Table 1. Considering the influences in all frequency ranges, five stiffness variables, five density variables, and the structural damping were selected as the calibration parameters, as listed in Table 4.

4.3 Model updating of the middle ear FE model

The middle ear FE model was updated using the proposed calibration framework with the selected calibration parameters. In the middle ear FE model, the controllable input (**x**) consists of the excitation frequency (f) only. The calibration metric for the calibration framework of Eq. (7) is defined as follows:

$$\Phi = \sum_{i=1}^{N_f} \phi(f_i), \tag{9}$$

where N_f is the number of selected frequencies for the model updating. The frequency selection was introduced in order to reduce the computational burden during the model updating. The center frequencies of the one-third octave bands were

Table 4. Calibrated parameters for the middle ear FE model.

Calibration parameters		Initial model (Logarithmic value)		Calibrated model (Logarithmic value)			
				Formulation I		Formulation II	
		Mean	SD	Mean	SD	Mean	SD
Stiffness	Malleus	$\log_{10}(1.2\times10^{10})$	1.008	$\log_{10}(3.499\times10^{10})$	0.8301	$\log_{10}(1.218\times10^{9})$	1.0298
	Incus	$\log_{10}(1.2\times10^{10})$	1.008	$\log_{10}(8.234\times10^{9})$	1.168	$\log_{10}(1.581\times10^{9})$	0.78348
	TM Ligament	$\log_{10}(6.0\times10^{5})$	0. 5778	$\log_{10}(1.003\times10^{6})$	0.5381	$\log_{10}(4.670\times10^{6})$	0.05103
	TM (Tensa)	$\log_{10}(3.34\times10^{7})$	0. 7524	$\log_{10}(2.871\times10^{8})$	0.5968	$\log_{10}(2.019\times10^{7})$	0.08988
	TM (Flaccida)	$\log_{10}(1.11\times10^{7})$	0. 7045	$\log_{10}(1.033\times10^{8})$	0.8305	$\log_{10}(9.988\times10^{7})$	0.32022
Structural damping		$\log_{10}(0.5\times10^{0})$	0.06021	$\log_{10}(1.080\times10^{0})$	0.06201	$\log_{10}(0.680\times10^{0})$	0.01092
Density	TM	$\log_{10}(1.2\times10^{3})$	0.1540	$\log_{10}(1.454\times10^{2})$	0.2886	$\log_{10}(1.563\times10^{2})$	0.30792
	Malleus (Head)	$\log_{10}(2.55\times10^{3})$	0.1703	$\log_{10}(2.563\times10^{3})$	0.1699	$\log_{10}(4.577\times10^{2})$	0.29744
	Malleus (Neck)	$\log_{10}(4.53\times10^{3})$	0.1784	$\log_{10}(4.719\times10^{2})$	0.1717	$\log_{10}(3.720\times10^{2})$	0.03414

selected for the validation metric.

Based on the ANOVA in the previous subsection, the selected input parameters for the calibration framework were defined as $\boldsymbol{\theta}_S = \{k_{\_Malleus}, k_{\_Incus}, k_{\_TM\ Lig.}, k_{\_TM(tensa)}, k_{\_TM(flaccida)}, k_{\_S.Damping}, \rho_{\_TM}, \rho_{\_Malleus(head)}, \rho_{\_Malleus(handle)}, \rho_{\_Incus(body)}, \rho_{\_Incus(LP)}\}$, where the variables k and ρ refer to the stiffness-related random variables in Table 2 and the density random variables in Table 3, respectively. The selected input parameters were assumed to be independent with respect to frequency. This assumption is very reasonable for the density variables; however, it is sometimes not reasonable for the stiffness-related parameters.

Two formulations for the bias FE model error were used in this study. In Formulation I, the bias FE model error was formulated as follows:

$$\delta(f) = \beta_0 + \beta_1 \cdot \log_{10} f \ . \tag{10}$$

It should be noted that, in Formulation I, the model error was estimated simultaneously with the other calibration input parameters. The simultaneous identification of the FE model errors in Formulation I has numerous advantages, such as in the completeness and generality of the formulation. However, when the calibration problem is solved under the minimization framework, the simultaneous identification formulation might cause a uniqueness problem in the solutions; that is, the objective function can be minimized by adjusting the calibration parameters with or without the FE model error. Calibrating the numerical model with the assumption of zero bias FE model error, a posterior calculation of the differences between the experimental data and calibrated model output provides an estimation of the FE model error. In order to investigate the non-uniqueness problem, the calibration process was repeated with the zero FE model error assumption, i.e. in the calibration parameter vector of Eq. (10), $\beta_0 = \beta_1 = 0$ was assumed: this is Formulation II. In Formulation II, the changes of the calibrated input parameters always include the compensation of the bias FE model error unless precise bounds for the variability of the input parameters are not given for the calibration framework. Comparing the calibrated parameters from Formulations I and II, the quality of the numerical model can be indirectly estimated: i.e., for high quality numerical model, it seems natural to expect nearly same calibrated parameters regardless of its formulations.

The minimization problem defined by Eqs. (6), (7) and (9) was solved using a MATLAB function ('fmincon') with a finite difference sensitivity calculation [32]. In the minimization problem of Eq. (7), the numbers of the calibration parameters were 25 and 23 for Formulations I and II, respectively. For the calculation of the calibration metric from 250 Hz to 10000 Hz, 17 one-third octave band center frequencies were selected. For the PDF estimations of the calibration metric, Eq. (9), the EDR method was used. In the PDF calculation, all variables listed in Tables 2 and 3, as well as the measurement errors, were considered as random variables: the number of random variables was 23 in total. Thus, one PDF calculation in the EDR method with 2N+1 scheme requests 47 analyses of the UDTF functions. The lower and upper bounds of the calibration parameters were set to 0.1 and 10 times the initial values, respectively. For the analysis, a PC workstation with two Intel Xeon QC CPUs and 24 GB RAM was used in 64-bit XP Windows operating system. The calculation time per objective function was 14 minutes in the PC workstation. The optimizer provided the results after 28 iterations and 781 function evaluations (Simulations) for formulation I, and after 84 iterations and 2526 function evaluations for formulation II. During the iterations, the objective function decreased by 89.2% from 247.1 to 26.65 for formulation I, and by 86% from 247.1 to 34.64 for formulation II. Figs. 7 and 9 present the statistical properties of the UDTFs (mean, 10%, and 90% CDF points) compared with those of the initial FE model and the measurement data for formulations I and II, respectively. In Table 4, the calibrated parameters are listed with the initial parameters. Figs. 7 and 9 demonstrate that the calibration framework moved the UDTF distributions of the initial FE model very close to the distributions of the experiments by adjusting the calibration parameters. The estimated FE model errors in the calibration process are also plotted in Figs. 7 and

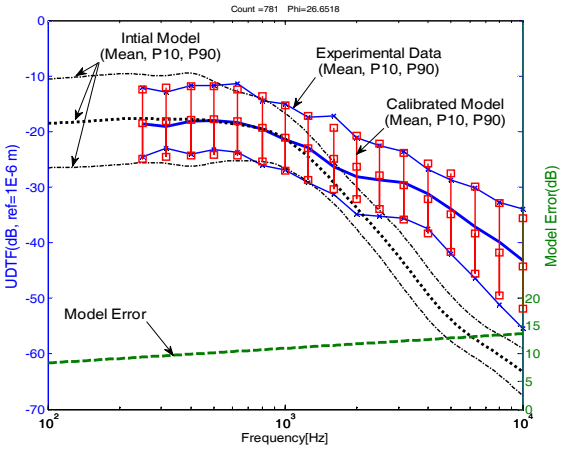

Fig. 7. UDTF calculated using the calibrated FE model (Formulation I).

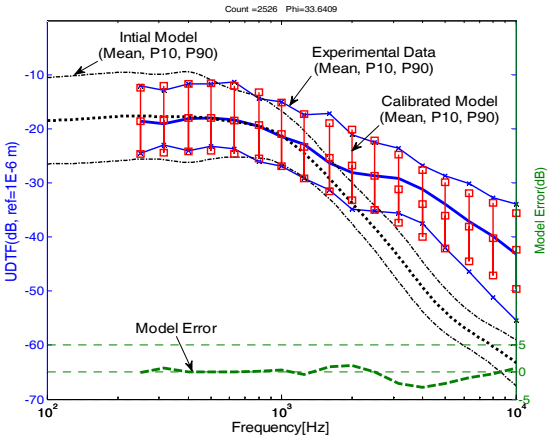

Fig. 9. UDTF calculated using the calibrated FE model (Formulation II).

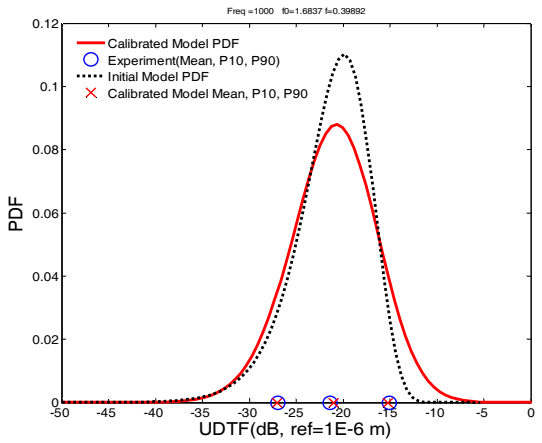

(a) 1000 Hz

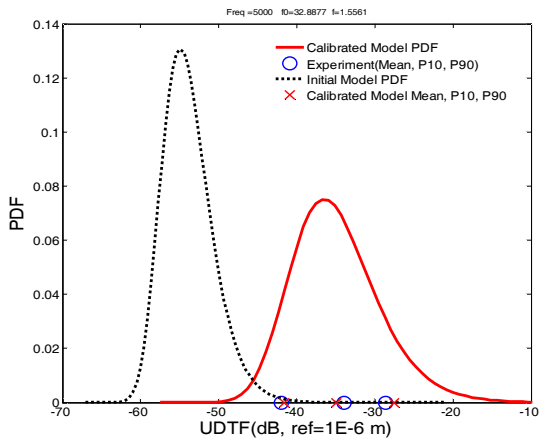

(b) 5000 Hz

Fig. 8. PDFs of the UDTF for the middle ear FE models: Formulation I (The markers represent the 10th, mean, and 90th percentiles for the calibrated (x) and experimental (Circle) results.

9 for formulations I and II, respectively. Note that the relatively large model error near 10 dB was included in the calibrated FE model for formulation I, which was identified simultaneously with the other calibration parameters. Thus, the initial FE model needed to move to a smaller magnitude in the UDTF on the lower frequency bands in formulation I. The model error in Formulation II was estimated through subtracting the mean values of the calibrated FE model from the measurement means at each frequency. In Fig. 8, the PDFs of the UDTF in the calibrated FE model for formulation I were compared with those in the initial FE model at two typical frequencies. At 1000 Hz, the optimization procedure changed the variability of the UDTF without significantly shifting the mean values. At a higher frequency range, both the mean and scattering of the UDTF were changed as shown in Fig. 8(b). It should be noted that the FE model errors were included in the PDFs in Fig. 8; that is, the UDTF variabilities were shifted by the amount of model error at the frequencies. Fig. 10 also presents the PDFs of the calibrated FE model for formulation II at two typical frequencies. Fig. 10 shows similar trends with those of formulation I in Fig. 8. Fig. 11 presents the improvements of the validation metric values through the calibration process for formulations I and II. The performances of the two calibrated models in Fig. 11 in terms of the validation metric were very similar. In higher frequency bands, the calibration framework decreased the discrepancy between the FE model and experimental data. In formulation I, the discrepancy was largely compensated by the model error, whereas in Formulation II largely by the means of the input parameters.

Through investigating the changes of the calibration input parameters for formulations I and II, it was found that the stiffness-related parameters of the incus decreased (i.e. became softer) and the density parameters of the malleus decreased (i.e. became lighter), whereas those of the tympanic membrane became stiffer and lighter. These trends may indicate updating directions for the true values of the material properties in a statistical sense. However, the specific calibrated input parameters are valid only in the FE models of this study because those values might include the contributions by the model errors and/or by the unidentified variability sources such as the variability of middle ear geometry. For example, A recent study for precise thickness distribution of tympanic

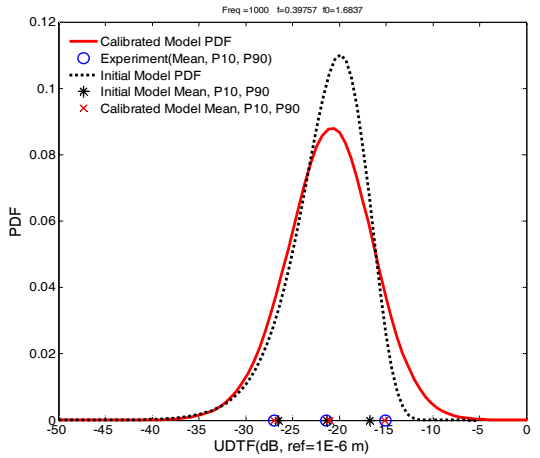

(a) 1000 Hz

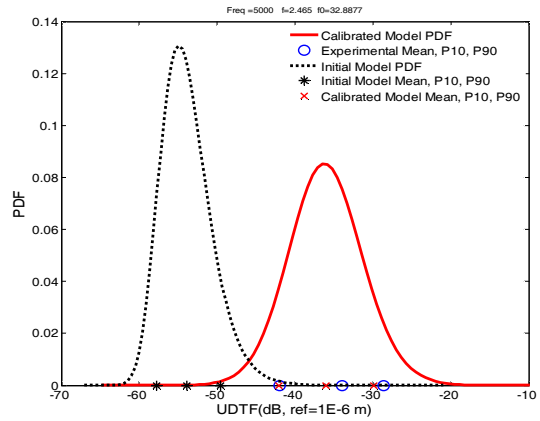

(b) 5000 Hz

Fig. 10. PDFs of the UDTF for the middle ear FE models: Formulation II (The markers represent the 10th, mean, and 90th percentiles for the initial (*), calibrated (x), and experimental (Circle) results.

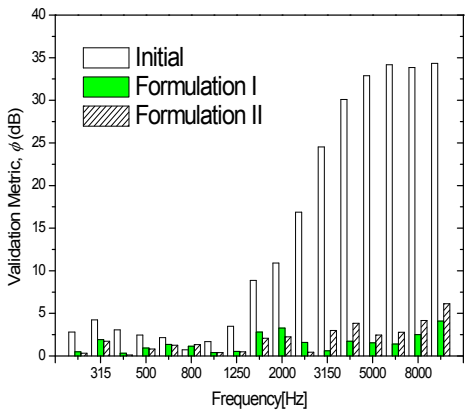

Fig. 11. Validation metrics for the calibrated FE models.

membrane [33] shows thinner thickness distribution than that of Ref. [5] which was used in this study, which partly explain the change of the calibrated input parameters for the tympanic membrane. The Ref. [33] also shows large geometric variability of the tympanic membranes along the subjects. Then, the calibrated input parameter may include these geometric variability since the experimental data used in the calibration framework were measured from different 99 subjects. It is suggested that for the identification of material properties using the proposed calibration framework, consistent geometry and experimental data acquisitions for a specific subject are desirable. As stated previously, to develop a method that can consider the geometric variability in a numerical model will be a challengeable topic in future research.

The results of formulation II appear better because the bias FE model errors were very small with the same variability assumptions for the material properties. Comparing the calibrated UDTFs of formulations I and II in Figs. 7 and 9, the FE model errors (δ) of Formulation II were much smaller than those of formulation I while the validation metric values (ϕ) are similar to each other as seen in Fig. 11. Accordingly, the calibrated parameter values differed significantly to each other. These results well demonstrate the uniqueness problem of the calibration framework. However, it cannot be known which formulation provides more close values to the true ones unless the material properties are measured accurately. This is a limitation of inverse approaches; yet, at the same time, the inverse approach is one of the best options that can be selected under these circumstances in order to enhance the model performance.

The calibration process generally requests a verification experiment [34]. In this study, the experimental data used in the calibration process were the PDF information extracted from large samples. Thus, the verification step would not be necessary in this study, which is another advantage of the proposed approach even though the proposed method is applicable when sufficient samples exist.

5. Conclusions

A statistical validation and model calibration procedure for a FE model of a human middle ear was proposed, taking into account the prescribed percentile values of the frequency responses at the umbo provided as experimental data. In order to assess the middle ear FE model, a statistical validation method based on the CDF interval comparison was introduced. The CDF intervals of the FE model were calculated using the EDR method. The comparison of the calculated CDF intervals with those of the prescribed experimental data exhibited good overview in the validity of the FE model along the frequency axis.

The proposed model calibration method minimized the sum of squares of the distances between the calculated and experimental responses at the prescribed percentiles in order to update the FE model input parameters. The calibration parameters were selected using an ANOVA for the input parameters of the middle ear FE model. The geometrical shapes and dimensions of the middle ear FE model were assumed to be deterministic because they were obtained from high precision CT scanning and individual variability of shapes was not ac-

counted for. The results of the ANOVA demonstrated the amount of contributions to the UDTF that results from the variabilities of the potential calibration parameters. Thus, the model calibration parameters could be easily selected, and this demonstrates the effectiveness of the proposed model calibration framework.

The model calibration framework was applied to the middle ear FE model with the selected calibration parameters and different model error formulations. It was found that the posterior model error estimation was better than the simultaneous estimation formulation. The FE model calibrated using the proposed method exhibited good agreement with the experimental data, which demonstrates the effectiveness of the statistical calibration method. However, the proposed calibration framework has non-uniqueness problem according to the model error formulations because of the limitation of inverse approach. The consideration of geometric variability for the middle ear FE model remains as future research. Furthermore, the efficiency in calculating the PDF sensitivity should be enhanced in future research.

Acknowledgment

This work was supported by a National Research Foundation (NRF) of Korea grant funded by the Korean government (MEST; grant no. 2010-0023464).

Nomenclature

ANOVA : Analysis of variance
CT : Computer tomography
CDF : Cumulative distribution function
COV : Coefficient of variation
EDR : Eigenvector dimension reduction
FE : Finite element
IM : Incudomalleolar
IS : Incudostapedial
LP : Long process
MCS : Monte Carlo simulation
MRI : Magnetic resonance imaging
PDF : Probability density function
TM : Tympanic membrane
UDTF : Umbo displacement transfer function

References

[1] S. E. Voss, J. J. Rosowski, S. N. Merchant and W. T. Peake, Acoustic responses of the human middle ear, *Hearing Research*, 150 (2000) 43-69.

[2] R. Aibara, J. T. Welsh, S. Puria and R. L. Goode, Human middle-ear sound transfer function and cochlear input impedance, *Hearing Research*, 152 (2001) 100-109.

[3] J. Pascal, A. Bourgeade, M. Lagier and C. Legros, Linear and nonlinear model of the human middle ear, *The Journal of the Acoustical Society of America*, 104 (1998) 1509-1516.

[4] G. Volandri, F. Di Puccio, P. Forte and S. Manetti, Model-oriented review and multi-body simulation of the ossicular chain of the human middle ear, *Medical Engineering & Physics* (2012).

[5] T. Koike, H. Wada and T. Kobayashi, Modeling of the human middle ear using the finite-element method, *The Journal of the Acoustical Society of America*, 111 (2002) 1306-1317.

[6] R. Gan, B. Reeves and X. Wang, Modeling of sound transmission from ear canal to cochlea, *Annals of Biomedical Engineering*, 35 (2007) 2180-2195.

[7] R. Z. Gan, Q. Sun, B. Feng and M. W. Wood, Acoustic-structural coupled finite element analysis for sound transmission in human ear--Pressure distributions, *Medical Engineering & Physics*, 28 (2006) 395-404.

[8] C.-F. Lee, P.-R. Chen, W.-J. Lee, J.-H. Chen and T.-C. Liu, Three-dimensional reconstruction and modeling of middle ear biomechanics by high-resolution computed tomography and finite element analysis, *The Laryngoscope*, 116 (2006) 711-716.

[9] T.-S. Ahn, M.-J. Baek and D. Lee, Experimental measurement of tympanic membrane response for finite element model validation of a human middle ear, *Springer Plus*, 2 (2013) 527.

[10] Y. M. Gal, M.-J. Baek and D. Lee, Finite element analysis of sound transfer characteristics for middle ear, *Transactions of the Korean Society of Mechanical Engineers A*, 35 (2011) 1563-1571.

[11] T. G. Trucano, L. P. Swiler, T. Igusa, W. L. Oberkampf and M. Pilch, Calibration, validation, and sensitivity analysis: What's what, *Reliability Engineering & System Safety*, 91 (2006) 1331-1357.

[12] B. D. Youn, B. C. Jung, Z. Xi, S. B. Kim and W. R. Lee, A hierarchical framework for statistical model calibration in engineering product development, *Computer Methods in Applied Mechanics and Engineering*, 200 (2011) 1421-1431.

[13] K. Campbell, Statistical calibration of computer simulations, *Reliability Engineering & System Safety*, 91 (2006) 1358-1363.

[14] M. C. Kennedy and A. O'Hagan, Bayesian calibration of computer models, *Journal of the Royal Statistical Society, Series B (Statistical Methodology)*, 63 (2001) 425-464.

[15] Y. Xiong, W. Chen, K.-L. Tsui and D. W. Apley, A better understanding of model updating strategies in validating engineering models, *Computer Methods in Applied Mechanics and Engineering*, 198 (2009) 1327-1337.

[16] H. B. Henninger, S. P. Reese, A. E. Anderson and J. A. Weiss, Validation of computational models in biomechanics, *Proceedings of the Institution of Mechanical Engineers, Part H: Journal of Engineering in Medicine*, 224 (2010) 801-812.

[17] A. E. Anderson, B. J. Ellis and J. A. Weiss, Verification, validation and sensitivity studies in computational biomechanics, *Computer Methods in Biomechanics and Biomedical Engineering*, 10 (2007) 171-184.

[18] D. Lee and T.-S. Ahn, A boundary element model for

acoustic responses in the ear canal and its statistical validation and updating, *Journal of Mechanical Science and Technology*, 28 (2014) 1203-1217.

[19] S. Nishihara and R. L. Goode, *Measurement of tympanic membrane vibration in 99 human ears*, in: H.t. KB (Ed.) Middle ear mechanics in research and otosurgery, Department of Oto-Rhino-Laryngology, Dresden, University of Technology, Dresden, Germany (1996) 91-93.

[20] C. J. Roy and W. L. Oberkampf, A comprehensive framework for verification, validation, and uncertainty quantification in scientific computing, *Computer Methods in Applied Mechanics and Engineering*, 200 (2011) 2131-2144.

[21] T. Cheng, C. Dai and R. Gan, Viscoelastic properties of human tympanic membrane, *Annals of Biomedical Engineering*, 35 (2007) 305-314.

[22] S. M. Hesabgar, H. Marshall, S. K. Agrawal, A. Samani and H. M. Ladak, Measuring the quasi-static Young's modulus of the eardrum using an indentation technique, *Hearing Research*, 263 (2010) 168-176.

[23] J. Aernouts, J. A. M. Soons and J. J. J. Dirckx, Quantification of tympanic membrane elasticity parameters from in situ point indentation measurements: Validation and preliminary study, *Hearing Research*, 263 (2010) 177-182.

[24] X. Zhang and R. Z. Gan, Dynamic properties of human tympanic membrane - experimental measurement and modelling analysis, *International Journal of Experimental and Computational Biomechanics*, 1 (2010) 252-270.

[25] N. Ghadarghadar, S. K. Agrawal, A. Samani and H. M. Ladak, Estimation of the quasi-static Young's modulus of the eardrum using a pressurization technique, *Computer Methods and Programs in Biomedicine*, 110 (2013) 231-239.

[26] R. Z. Gan, F. Yang, X. Zhang and D. Nakmali, Mechanical properties of stapedial annular ligament, *Medical Engineering & Physics*, 33 (2011) 330-339.

[27] B. Youn, Z. Xi and P. Wang, Eigenvector dimension reduction (EDR) method for sensitivity-free probability analysis, *Structural and Multidisciplinary Optimization*, 37 (2008) 13-28.

[28] B. C. Jung, D. Lee, B. D. Youn and S. Lee, A statistical characterization method for damping material properties and its application to structural-acoustic system design, *The Journal of Mechanical Science and Technology*, 25 (2011) 1893-1904.

[29] S. Wang, W. Chen and K.-L. Tsui, Bayesian validation of computer models, *Technometrics*, 51 (2009) 439-451.

[30] R. Roy, *A primer on the Taguchi method*, Van Norstrand Reinhold, New York (1990).

[31] L. Qi, C. S. Mikhael and W. R. J. Funnell, Application of the Taguchi method to sensitivity analysis of a middle-ear finite-element model, *Proc. 28th Ann. Conf. Can. Med. Biol. Eng. Soc*. (2004) 153-156.

[32] The Mathworks Inc., *Optimization toolbox user's guide : For Use with MATLAB*, The Mathworks Inc., Natick, MA 01760-2098, USA (2000).

[33] S. Van der Jeught, J. J. Dirckx, J. R. Aerts, A. Bradu, A. G. Podoleanu and J. A. Buytaert, Full-field thickness distribution of human tympanic membrane obtained with optical coherence tomography, *JARO*, 14 (2013) 483-494.

[34] W. L. Oberkampf and C. J. Roy, *Verification and validation in scientific computing*, Cambridge University Press, Cambridge (2010).

Dooho Lee received his B.S. degree from Seoul National University (Korea) in 1988, his M.S. from KAIST (Korea) in 1990, and his Ph.D. from KAIST (Korea) in 1994. He worked for Samsung Motors, Inc. (1995-1999), and is currently a professor in Dongeui University. His research focuses on the design optimization of structural-acoustic systems, uncertainty propagation in dynamic problems, and sound transfer characteristics in human hearing systems.

Tae-Soo Ahn received his B.S., M.S. and Ph.D. degrees in Mechanical Engineering from Dongeui University, Korea in 2005, 2008, and 2012, respectively. He is a researcher in SEGI Engineering Inc., Korea. He has an interest in NVH system measurements and the sound transfer characteristics in human hearing system.